


Modulating antibiotic release from reservoirs in 3D-printed orthopedic devices to treat periprosthetic joint infection

Brian Allen¹  | Christina Moore² | Thorsten Seyler² | Ken Gall¹

¹Department of Mechanical Engineering and Materials Science, Edmund T. Pratt Jr. School of Engineering, Duke University, Durham, North Carolina

²Department of Orthopaedic Surgery, Duke University Medical Center, Durham, North Carolina

Correspondence

Brian Allen, Department of Mechanical Engineering and Materials Science, Edmund T. Pratt Jr. School of Engineering, Duke University, 144 Hudson Hall, Box 90300, Durham, NC 27708.
Email: bwa6@duke.edu

Funding information

Duke University, Grant/Award Number: 291-0067

Abstract

Periprosthetic joint infection is a costly debilitating affliction following total joint arthroplasty. Despite a relatively low incidence rate, periprosthetic joint infection is an increasing problem due to a substantial increase in arthroplasty surgeries over time. The current treatment is replacing the primary implant with a temporary bone cement spacer that releases antibiotics over time. However, the spacer is mechanically weak with an ineffective antibiotic release. Alternatively, three-dimensional (3D)-printed reservoirs in high-strength devices have the potential to release antibiotics long term in a controlled manner. In this study, 3D-printed reservoirs were loaded with calcium sulfate embedded with gentamicin. In vitro antibiotic release is tuned by varying reservoir parameters, such as channel length, diameter, and quantity. In addition, a straightforward computational model effectively predicts antibiotic release curves to rapidly design devices with a preferred release profile. Overall, this study highlights a novel approach to potentially develop high-strength joint implants with the long-term effective release of antibiotics to treat the periprosthetic joint infection.

KEYWORDS

3D printing, elution study, periprosthetic joint infection, revision surgery, total joint arthroplasty

1 | INTRODUCTION

Periprosthetic joint infection (PJI) is an infection, most commonly by *Staphylococcus aureus*, near a synthetic implant in the surrounding tissue following total joint arthroplasty (TJA).¹ The infection rate for TJA ranges from 1% to 4%,² although the rate is even higher for the revision of a failed TJA, possibly due to prolonged operating time.¹ Since the number of orthopedic operations performed annually in the US is increasing due to an aging population, the number of infections is steadily rising over time.³ High costs associated with hospitalization for infected implants exert an enormous financial burden on the US health care system. The annual cost of revision procedures for infected knee and hip implants in the US increased from \$320 million in 2001 to \$566 million in 2009 and is projected to exceed \$1.62 billion by 2020.⁴

The current treatment for infected implants is an expensive multistage approach that begins with the removal of the implant and thorough debridement of infected tissue followed by the administration of systemic and locally delivered antibiotics, which can be achieved by implantation of an orthopedic device, such as a spacer or beads, embedded with antibiotics.^{5,6} The gold standard biomaterial is poly(methyl methacrylate) (PMMA) bone cement “spacers” designed to fill the implant void site and provide temporary mechanical stability during drug elution.⁷ However, PMMA has many limitations, including (a) poor antibiotic release rates, (b) limited number of compatible antibiotics due to a damaging exothermic reaction during cement setting, (c) weak mechanical properties that prevent reasonable levels of load-bearing activity, and (d) need for a follow-up surgery to remove the nonbiodegradable PMMA.⁸⁻¹⁰ Antibiotics have a small surface-mediated burst release from PMMA in the first

24 hours followed by a subtherapeutic release for many years thereafter.^{11,12} Since only a small fraction of antibiotic elutes from the spacers, high concentrations of antibiotics are required.^{12,13} This leads to profound reductions in mechanical strength, leading to frequent breaking of the spacer, which is a painful and costly consequence.¹⁴

Alternative biomaterials to PMMA include bioceramics, especially calcium sulfate (CS) and calcium phosphates (CPs). These materials release antibiotics more effectively than PMMA and are biodegradable.¹⁵⁻¹⁷ In addition, there is no exothermic reaction involved in cement hardening, which enables the use of a wider range of antibiotics than is possible with PMMA. Numerous studies have demonstrated the potential of bioceramics as a depot for antibiotic delivery.^{15,16,18-23} However, bioceramics have significantly weaker mechanical properties than PMMA, preventing their use in load-bearing implants, such as knee and hip spacers. Overall, current treatment options lack both the mechanical strength and elution kinetics to effectively treat bone infections while bearing high-mechanical loads.

In addition to injection molding or machining, three-dimensional (3D) printing is another relatively new technique used to fabricate orthopedic implants. One study examined 3D-printed antibiotic-laden calcium phosphate cements (CPCs) to treat a mouse model of infection.¹⁶ The 3D-printed CPC significantly reduced the bacterial burden compared to the antibiotic-loaded PMMA control. However, the mouse model does not require a high-strength material compared to infected implant sites in humans. On the other hand, a few studies used a metal 3D-printing technique called selective-laser melting (SLM) to make high-strength implants containing a hollow reservoir connected to the surroundings by channels. A major advantage of 3D printing is the ability to create reservoirs with complex internal geometries that cannot otherwise be created with conventional manufacturing methods. One study loaded an antibiotic-impregnated CPC into titanium cylinders with an inner reservoir.²⁴ The antibiotic release profiles could be tuned by modulating the orientation of the channels. Another study covered channels in 3D-printed hollow titanium cubes with polymer membranes to extend release.²⁵ A third study manipulated SLM printing settings to change the porosity of titanium.²⁶ Antibiotic release was extended as the porosity of the titanium decreased. These studies demonstrate a proof-of-concept that modulating reservoir geometry can tune the drug release profile. However, these studies were limited in scope and only demonstrated the release of antibiotics for less than 24 hours, which is insufficient to eliminate an infection. A more comprehensive study of reservoir geometry is needed to optimize the release of antibiotics for many weeks to effectively treat PJI.

In this study, a photocured rigid polyurethane (RPU 60) was selected as a prototyping material for 3D-printing devices with internal reservoirs, loaded with calcium sulfate hemihydrate (CSH) and gentamicin. Varying channel parameters, such as quantity, diameter, and length, had a significant effect on the *in vitro* elution kinetics of gentamicin. A computational model of gentamicin release from reservoirs can expedite the design of devices with desired antibiotic

release profiles. Overall, this study demonstrates the long-term release of antibiotics with high-strength devices to effectively treat PJI.

2 | MATERIALS AND METHODS

2.1 | Materials

The materials used for this study include CSH and gentamicin sulfate powders that were purchased from Sigma-Aldrich. Photocured chemically cross-linked RPU 60 resin was purchased from Carbon 3D. The RPU 60 resin is 3D printed into cube-shaped reservoirs using the M1 printer from Carbon 3D via continuous liquid interface production. After 3D printing, the reservoirs are thoroughly washed with isopropanol and then cured in a convection oven at 120°C for 4 hours. Low-viscosity PMMA bone cement containing gentamicin (PALACOS LV+G) was obtained (Zimmer-Biomet). *S. aureus* strain 29213 from American Type Culture Collection (ATCC) was used for bacterial studies. Mueller-Hinton Broth 2 was purchased from Sigma-Aldrich and Tryptic Soy Broth was purchased from BD Bacto. Six millimeters Whatman antibiotic discs were also purchased from Sigma-Aldrich.

2.2 | Loading reservoirs and elution study

Cube-shaped reservoirs were designed with an outer shell (2 mm thick) made of RPU 60 with a large inner volume (20 mm side dimension) (Figure 1A). Channels can be designed in the shell of the reservoir to connect the inner volume to the surroundings. A port for syringe injection is located on the top face of the cube to load cement embedded with gentamicin.

Figure 1B illustrates the experimental design for studies to assess the elution kinetics of gentamicin from the reservoirs. Reservoirs were loaded with cement composed of CSH, deionized water, and gentamicin sulfate at a ratio of 2 g/1 mL/80 mg, respectively. The sides of the reservoirs containing channels were tightly wrapped with parafilm to reduce leakage during cement loading. A custom-designed cap was glued into the opening at the top of the reservoir to prevent the unwanted gentamicin elution. The cement set for at least 2 hours prior to starting the elution study. The mass of the reservoir was recorded before and after loading. Control blocks of CSH cement (20 × 20 mm²) were prepared using the same ratio of CSH, water, and gentamicin sulfate. The cement paste was injected via syringe into a custom-designed mold made of multiple pieces that could be separated to release the block after setting for at least 2 hours. PALACOS LV+G was prepared according to the manufacturer's instructions and injected into the mold. The pieces of the mold were cut away to obtain the block of cement.

The samples were then fully submerged in 0.9% NaCl solution. Throughout the experiment, the samples were maintained at 37°C. At each time point, the saline was passed through a 0.22 μm filter,

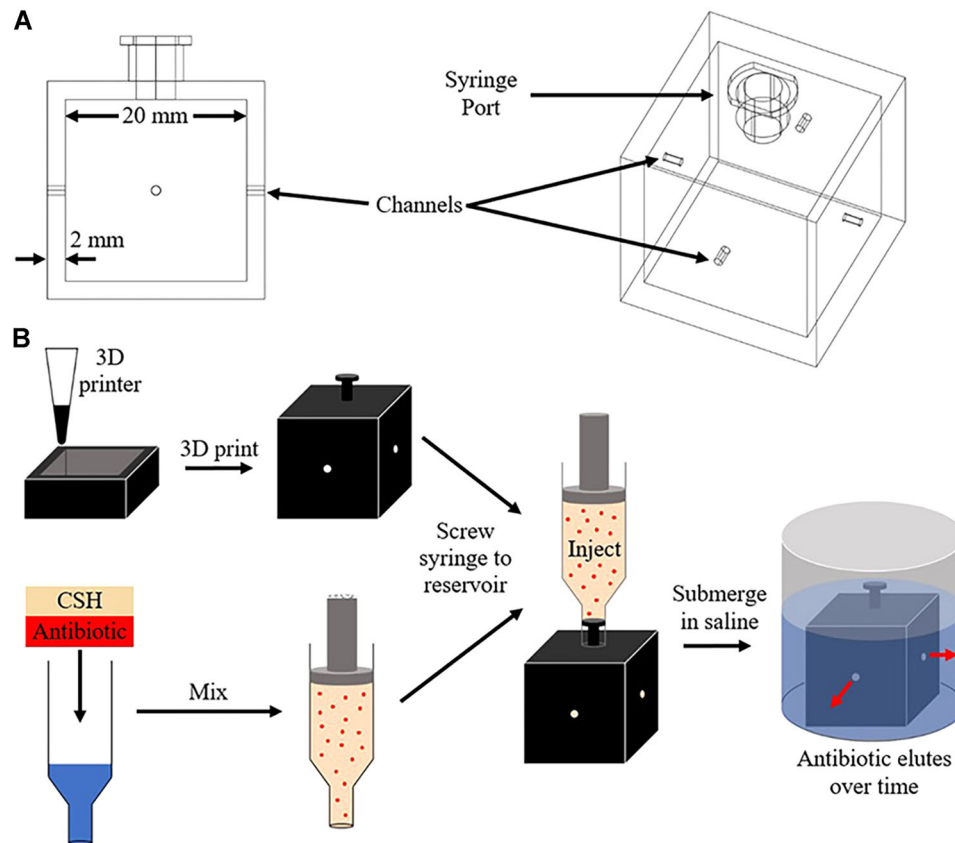


FIGURE 1 Experimental Design. A, Reservoirs are cube-shaped with an inner side dimension of 20 mm and a wall thickness of 2 mm. There are channels on the four sidewalls and a syringe port on top. B, Reservoirs are 3D printed from RPU prototyping material. CSH and gentamicin powders are mixed with water to form a paste and injected into the reservoirs. After the cement setting, reservoirs are submerged in saline, which is collected at various time points to measure antibiotic concentration. 3D, three dimensional; CSH, calcium sulfate hemihydrate; RPU, rigid polyurethane [Color figure can be viewed at wileyonlinelibrary.com]

and a small sample was collected to measure the concentration of gentamicin. The saline was completely replaced at each time point.

2.3 | Disk diffusion assay

The concentration of gentamicin in each sample was assessed using a disk diffusion assay according to methods recommended by the Clinical and Laboratory Standards Institute (CLSI). Briefly, the *S. aureus* inoculum density was standardized to a 0.5 McFarland standard. A hundred microliters of the culture were coated evenly across the surface of a Mueller-Hinton agar plate using a sterile spreader. Fifteen microliters of samples containing gentamicin were loaded onto 6-mm Whatman antibiotic assay discs. The discs were placed onto agar plates and incubated at 37°C overnight. Zones of inhibition (ZOI) where bacteria are unable to grow around the disks (see Figure S1A). The plates were imaged and diameters of the ZOI's were determined using the ImageJ software. The diameter of the ZOI is approximately proportional to the logarithm of the gentamicin concentration (see Figure S1B). The minimum ZOI is 6 mm since that is the disk diameter.

2.4 | Approximate cumulative release

Serial dilutions of known concentrations of gentamicin were tested in a disk diffusion assay to get a standard curve of concentration vs ZOI. A line of best fit was determined with the formula: $ZOI = 2.528 \times \ln(\text{concentration}) - 0.2034$ with $R^2 = .9892$. Approximate gentamicin concentrations were determined from ZOI values from elution studies. To get the approximate total gentamicin released, the concentrations were multiplied by the volume of saline. Approximate cumulative release curves were determined by summing the approximate gentamicin quantities released at each time point over time.

2.5 | Broth dilution assay

The minimum inhibitory concentration (MIC) of gentamicin was determined using a broth dilution assay according to the methods recommended by the CLSI. Briefly, an overnight culture of *S. aureus* (ATCC 29213) was diluted to a 0.5 McFarland standard. The bacterial concentration was serially diluted in cation-adjusted Mueller-Hinton

broth (CAMHB) to reach an inoculum concentration of 1×10^6 colony-forming units (CFUs)/mL. Two-hundred microliters of CAMHB were added to 96-well plates as a sterile control. CAMHB of concentration 180 μ L and inoculum of 20 μ L were added to the 96-well plates as a growth control to get a final concentration of 1×10^5 CFUs/mL. To test the concentration of samples containing gentamicin, 80 μ L of CAMHB, 20 μ L of inoculum, and 100 μ L of the sample was added to the 96-well plates. The plate was incubated at 37°C overnight for 16 to 20 hours. The optical density at 600 nm was measured the next day. The MIC for *S. aureus* 29213 is approximately 2.5 μ g/mL (see Figure S1C).

2.6 | Compression testing

For mechanical testing, the reservoirs were 3D printed without the top and bottom faces so that only the four vertically facing walls were 3D printed. The compressive strength of the reservoirs was measured using a Test Resources 830LE63 Axial Torsion Test Machine equipped with a 10 000-lb load cell. The displacement rate was maintained at 1 mm/min. The compressive strength was calculated as the maximum load divided by the cross-sectional area. The Young's modulus was calculated as the slope of the linear portion of the stress-strain curve.

2.7 | Statistics analysis

For graphs of ZOI and cumulative release curves, full-factorial repeated measures analysis of variance was used to test significance. For nonlinear relationships, the data were linearized with a log transform to perform an analysis of covariance unequal slopes to determine the statistical significance. Most conditions are $n = 3$ to 5, but some conditions were reduced to $n = 2$ due to human error. $P < .05$ is considered as significant. Error bars reported in figure graphs are represented as the standard error of the mean.

3 | RESULTS

To treat bone infections caused by *S. aureus* and other pathogens, PMMA and CSH are two common biomaterials used as a depot for local antibiotic delivery.¹⁰ PALACOS LV+G is a PMMA-based bone cement containing gentamicin with a low viscosity so it can be injected with a syringe. PALACOS LV+G (40:1 g ratio of PMMA:gentamicin) and CSH (40:1.6 g ratio of CSH:gentamicin) were loaded into custom-designed molds to make cubes with a 20 mm side dimension (Figure 2A). These control cubes were compared to reservoirs loaded with CSH (40:1.6 g ratio of CSH:gentamicin) with one channel (0.5 mm diameter) on each vertically facing side. In agreement with previous reports,^{27,28} therapeutic levels of gentamicin released over longer periods of time from CSH than PMMA (Figure 2B). There was an initial burst release of gentamicin from PMMA in the first 24 hours with only

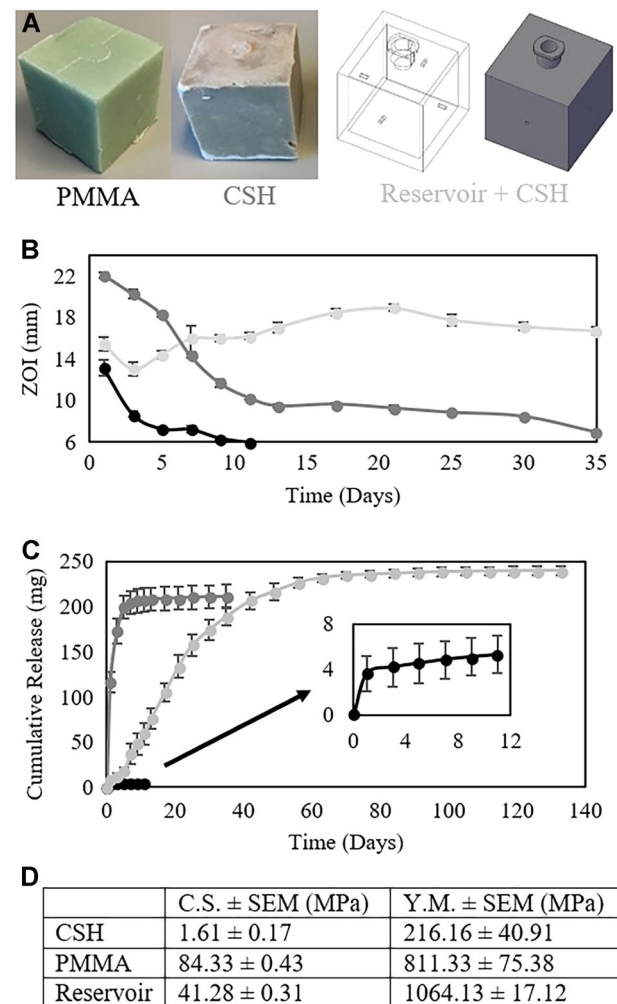


FIGURE 2 Reservoirs extend antibiotic release. A, Representative images of PALACOS LV+G PMMA cement (left), calcium sulfate with gentamicin (center), and a schematic of reservoirs loaded with calcium sulfate/gentamicin. B, ZOI vs time for these conditions. The colors of the words in (A) correspond to the colors in the graphs. C, Cumulative release vs time. Reservoirs extend release vs CSH and PMMA alone ($P < .0001$). D, Compressive strength and Young's modulus. Reservoirs improve the strength of CSH alone ($P < .0001$). CS, compressive strength; CSH, calcium sulfate hemihydrate; PMMA, poly(methyl methacrylate); YM, Young's modulus; ZOI, zones of inhibition [Color figure can be viewed at wileyonlinelibrary.com]

minimal release thereafter. There was a burst release of gentamicin from CSH in the first 5 days and steady release of low gentamicin levels over the next four weeks. CSH released significantly more antibiotics than PMMA (204.17 ± 8.10 vs 5.31 ± 0.96 mg; $P < .0001$) (Figure 2C). Importantly, the reservoir loaded with CSH released therapeutic levels of gentamicin significantly longer than CSH or PMMA alone ($P < .0001$) (Figure 2B,C). Despite more favorable release kinetics, CSH had a significantly lower compressive strength (1.61 ± 0.17 vs 84.33 ± 0.43 MPa; $P < .0001$) and Young's modulus (216.16 ± 40.91 vs 811.33 ± 75.38 MPa; $P < .01$) than PMMA (Figure 2D). In addition to extending antibiotic release, the reservoir

significantly improved the strength of CSH (41.28 ± 0.31 vs 1.61 ± 0.17 MPa; $P < .0001$), although with a lower compressive strength than PMMA (41.28 ± 0.31 vs 84.33 ± 0.43 MPa; $P < .0001$) since RPU is a relatively weak prototyping material. Stronger 3D-printable materials, such as titanium or cobalt-chrome, would have a significantly greater compressive strength than PMMA. The results in Figure 2 demonstrate that PMMA is relatively strong but cannot effectively release antibiotics, while CSH is an effective release matrix but almost two orders of magnitude weaker than PMMA. The combination of CSH with a printed scaffold provides better potential elution and strength than either PMMA or CSH alone.

Further studies were performed to determine the effect of channel geometry on gentamicin elution. The diameter of the channel ranged from 0.5 to 15 mm (Figure 3A). The channel porosity, which is the percent area of one side of the inner reservoir that is exposed to channels, varied from 0.05% to 44.18%. Decreasing the channel diameter significantly prolonged gentamicin release ($P < .0001$) (Figure 3B,C). There was a detectable ZOI for at least 90 days with the lowest diameter, approximately 13-fold longer than PMMA.

Another way to tune porosity is the number of channels. Reservoirs with different channel numbers (1 mm diameter) were loaded with CSH and gentamicin (Figure 4A). The number of channels ranged from 1 to 25 channels per side and the porosity varied from 0.2% to 4.91%. The duration of elution was extended at low porosities (Figure 4B). Reservoirs with one channel per side had greater elution after 3 weeks than reservoirs with multiple channels per side ($P < .0001$). There was no significant difference among reservoirs with multiple channels per side.

To further understand the relative importance of channel porosity distribution on elution kinetics, reservoirs with the same channel porosity (~20%) but different channel number and diameter were studied (Figure 4D). There was no significant difference in antibiotic release among reservoirs with constant porosity (Figure 4E,F). There was a slight but not significant increase in elution by reservoirs with one channel, possibly due to the reduced dispersion of porosity across the face of the reservoir (see Figure S2). For reservoirs with one channel, the reservoir corner is nearly 10 mm away from the closest channel. As the number of channels increases, the distance from corner to channel decreases sharply. Combining the data from all of these studies show that there is, in fact, a significant difference between single and multiple channels at lower porosities (Figure 4G).

To further tune antibiotic elution, 3D printing enables the design of complex structures to modify channel length. Channels were 3D printed with greater lengths extending into the reservoirs (Figure 5A). These new structures extended the length from 2 to 7 mm (0.5 mm diameter). Increasing the length significantly increased the duration of the gentamicin release ($P < .001$) (Figure 5B). Reservoirs with a 7-mm channel length released gentamicin for longer than 180 days, the duration for which spacers are cleared for use in patients (Figure 5C). Reservoirs with the longer channels released 90% of gentamicin by 186.67 ± 9.33 vs 47.60 ± 4.08 days by reservoirs with 2-mm channel length (Figure 5D). However, this

channel design has two limitations. First, the channels extend into the reservoir, which reduces the amount of cement that can be loaded (9.79 ± 0.18 vs 12.53 ± 0.08 g; $P < .0001$) (see Figure S3) and the total amount of antibiotics released (156.27 ± 5.74 vs 240.25 ± 4.67 g; $P < .0001$) (Figure 5D). Second, there is only one small channel per side, which could potentially limit the dispersion of antibiotics throughout the surrounding tissue following implantation.

These limitations can be overcome by designing reservoirs with channels embedded within the shell of the reservoir (Figure 5E). Channels (1 mm diameter) were designed in an "X-shaped" pattern. Gentamicin in the reservoir enters the channel network through a single opening at the center of the "X." The lengths of the four channels that compose the X-shape can be varied (0 to 4 to 12 mm) to modulate the release profile, and the gentamicin exits to the surroundings at the four ends. With this design, there are no structures in the inner volume that limit the amount of cement, and multiple exits from the channel network could improve the dispersion of gentamicin to the surroundings. Increasing the length of the channels significantly extended the gentamicin release ($P < .0001$) (Figure 5F,G).

To better understand the role of reservoir geometry on gentamicin elution, a computational model was developed. The reservoirs were modeled as a 3D matrix in MATLAB (Figure 6A). "Antibiotics" are randomly distributed throughout the matrix, diffuse via a random walk, and leave the matrix at designated "exits" at the ends of channels. To simulate degradation, the exit entries of the matrix shift inward over time (Figure 6B). The model parameters for gentamicin diffusion and CSH degradation were determined by fitting the model

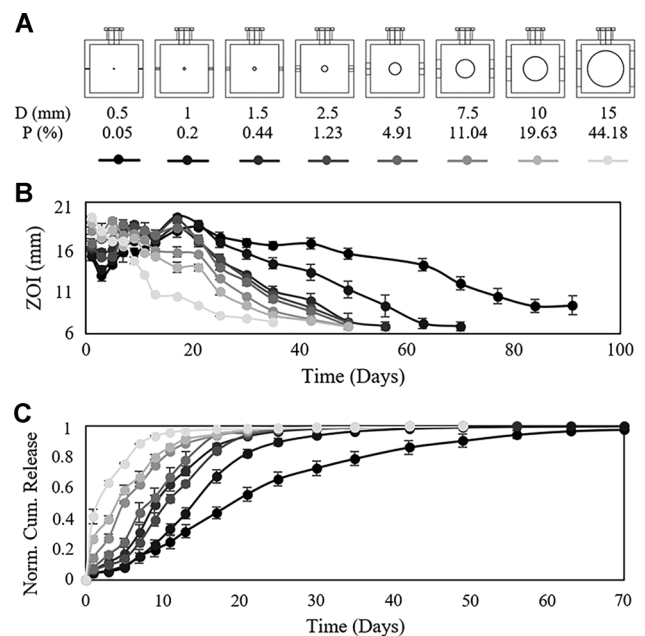


FIGURE 3 Effect of channel diameter on antibiotic release. A, Schematic of reservoirs with a varying diameter (D) and porosity (P). B, ZOI vs time for varying diameters. C, Normalized cumulative release over time. Decreasing channel diameter extends release ($P < .0001$). ZOI, zones of inhibition

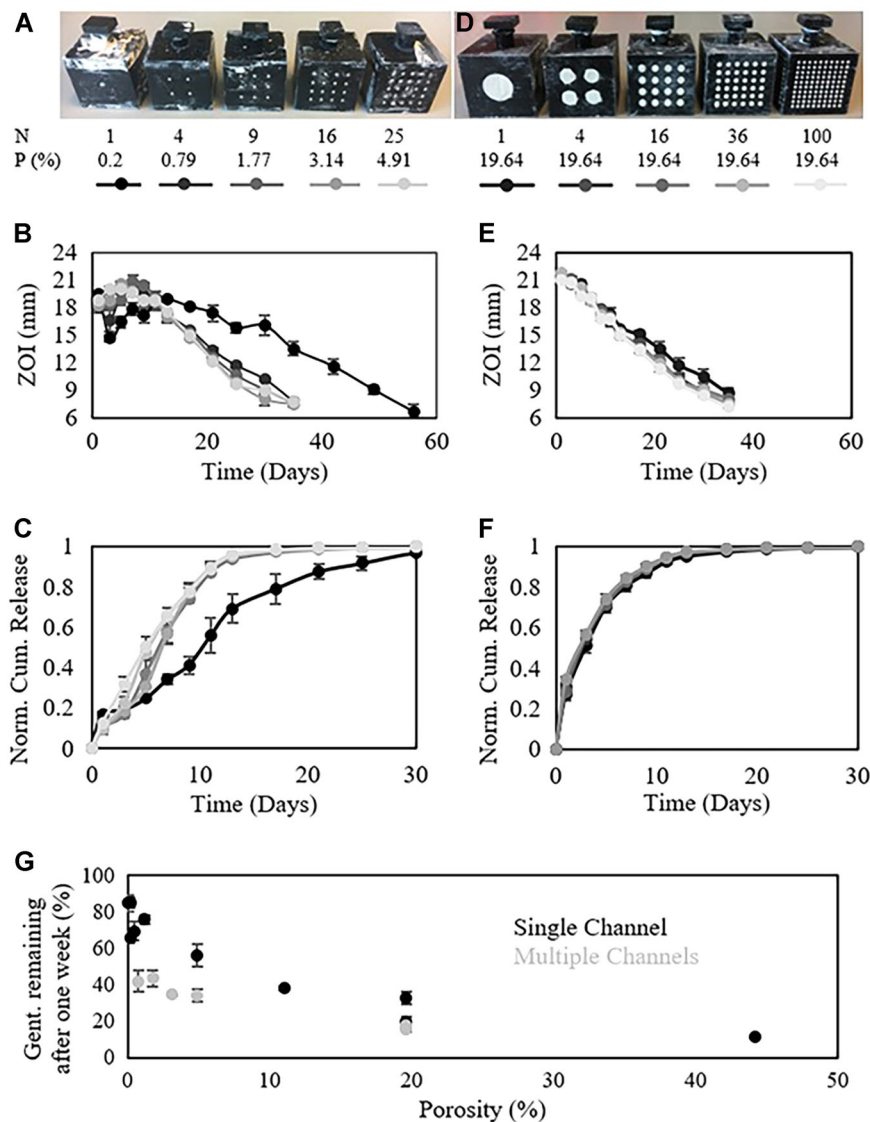


FIGURE 4 Effect of channel number of the antibiotic release. A, Image of reservoirs with varying channel number (N) and porosity (P) with a constant diameter of 1 mm. B, ZOI vs time for reservoirs in (A). C, Normalized cumulative release calculated from (B) vs time. Reservoirs with one channel per side have extended release compared to reservoirs with multiple channels per side ($P < .0001$). D, Image of reservoirs with varying channel numbers but constant porosity. E, ZOI vs time for reservoirs in (D). F, Normalized cumulative release calculated from (E) vs time. There is no significant difference among conditions. G, Percent of gentamicin remaining in reservoirs after 1 week as a function of porosity for reservoirs in Figures 3 and 4. The percent remaining decreases significantly as porosity increases ($P < .0001$), and there is a significant downward shift for reservoirs with multiple channels per side ($P < .0001$). ZOI, zones of inhibition [Color figure can be viewed at wileyonlinelibrary.com]

to the cumulative release curves of the experimental data. The model provided a reasonable fit for gentamicin release from reservoirs with large diameters (≥ 2.5 mm) (Figure 7A) but not small diameters (≤ 1.5 mm) (Figure 7B). Furthermore, the model did not accurately fit the experimental data for reservoirs with longer channel lengths with small diameters (Figure 7C). There are three possible explanations for a poor model fit at small diameters: (a) the saline cannot effectively pass through small channels due to the hydrophobicity of the RPU, (b) degraded cement cannot pass through the small channels, or (c) the model does not accurately reflect the mechanism of gentamicin elution from reservoirs.

To test the first hypothesis, cylinders were 3D printed with channels of varying diameter (Figure S4). Saline was slowly added to the cylinders until it flowed through the channels. Greater height of saline was needed to flow through channels with smaller diameters (Figure 8). In fact, the three smallest diameters require a larger saline height than was used in the elution study, which could potentially explain why the model poorly fit the data for these diameters.

Therefore, the effect of the saline height on gentamicin elution was studied for two-channel diameters: 0.5 mm, which was the smallest diameter tested previously, and 8 mm, for which the model predicts an approximately linear cumulative release curve. The reservoirs were tested at saline heights of about 12 and 35 mm. There was not a significant effect of saline height for reservoirs with the larger diameter, but the larger saline height significantly expedited gentamicin elution for reservoirs with the smaller channel diameter ($P < .01$) (Figure 9A). However, the model still did not accurately fit the data for reservoirs with the 0.5-mm channel diameter. To potentially explain this, the reservoir mass was tracked over the course of the elution study (Figure 9B). There was a significantly greater increase in mass after 24 hours for reservoirs with the larger channel diameter due to a greater influx of saline into the porous cement, suggesting the saline still cannot effectively penetrate the smaller channels. The mass of the reservoirs with smaller channels continued to increase over time as the saline slowly penetrated the channels over time. On the other hand, the mass of reservoirs with larger

FIGURE 5 Effect of channel length on antibiotic release. A, Schematic of reservoirs with varying channel length. B, ZOI vs time for reservoirs in (A). The color of the labels in (A) corresponds to the colors of the curves. C, Cumulative release calculated from (B) vs time. D, Table of values for the time needed for 90% of gentamicin release (T_{90}) and total gentamicin released (Gent.). Increasing channel length prolongs release ($P < .0001$) but decreases Gent. ($P < .0001$). E, schematic of reservoirs with “X-shaped” channels in the reservoir walls. F, ZOI vs time for reservoirs in (E). The color of the labels in (E) corresponds to the colors of the curves. G, Cumulative release calculated from (F) vs time. H, Table of values for T_{90} and Gent. Twelve-millimeter channel length prolongs release ($P < .0001$) without a significant effect on total gentamicin released. ZOI, zones of inhibition

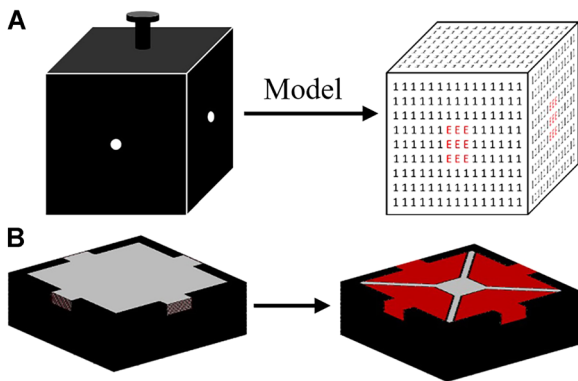
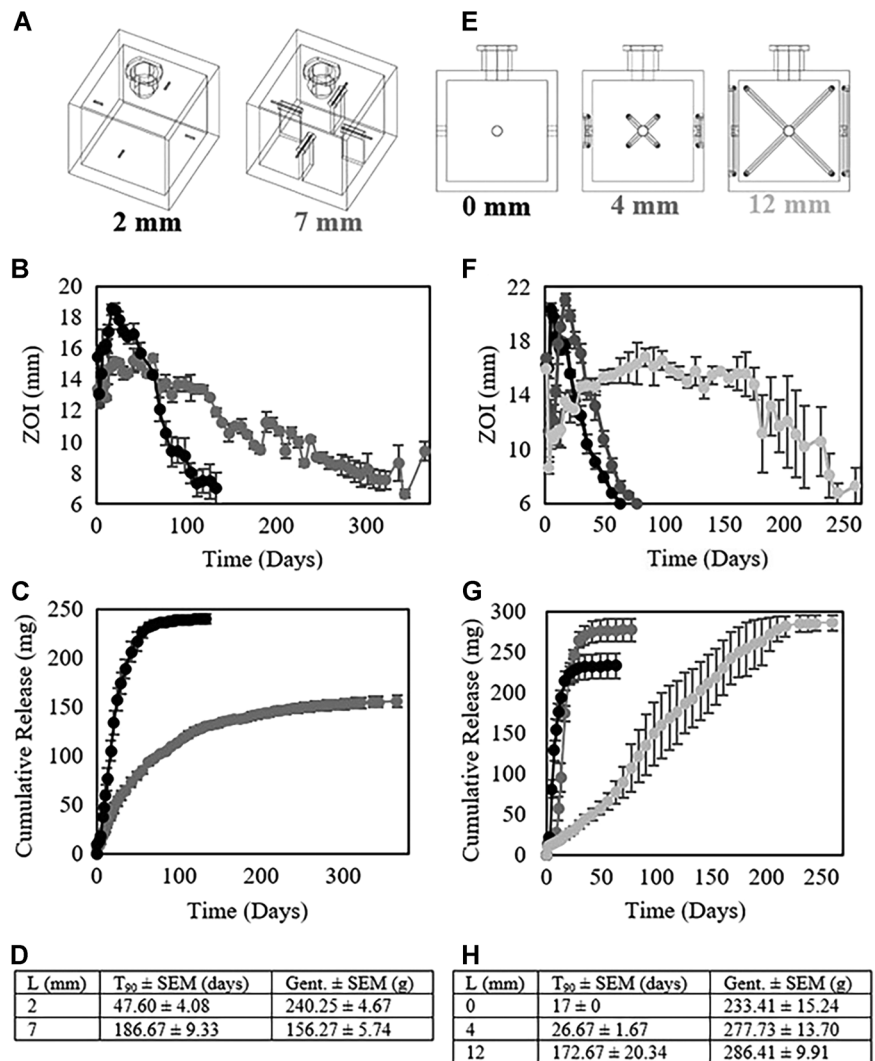


FIGURE 6 A computational model of gentamicin released from reservoirs. A, The cube-shaped reservoir (left) is modeled as a 3D matrix (right) in MATLAB. Matrix entries are modified to create reservoir geometry. In the schematic, the red “E” entries represent the channel exits and the “1” entries represent the carrier. B, The computational model incorporates surface degradation of the cement. Black represents the reservoir. Gray represents the carrier. Red represents a degraded carrier. The images show degradation at time 0 (left) and a later time point (right). 3D, three dimensional [Color figure can be viewed at wileyonlinelibrary.com]

channels decreased over time due to cement degradation. This loss was greater for reservoirs with higher saline heights, which suggests that increasing the pressure of saline on the cement increased the degradation rate. Although the model does not accurately predict gentamicin release for reservoirs with small channel diameters, the model accurately predicted that a channel diameter of 8 mm would result in an approximately linear cumulative release curve over a range of channel lengths (Figure 9C).

In addition to elution kinetics, channel porosity could also influence mechanical properties. Video S1 shows a representative time-lapse video of compression testing. Increasing porosity significantly decreased the compressive strength and Young's modulus ($P < .0001$) (Figure 10A,B). Figure 10C shows representative stress/strain curves for reservoirs with a range of porosities. Despite affecting gentamicin release, the number of channels per side did not significantly affect the compressive strength but does have a slight but significant effect on Young's modulus ($P < .01$). Decreasing porosity both extended gentamicin release and increases the compressive strength ($P < .0001$) (Figure 10D). This could be advantageous for load-bearing devices

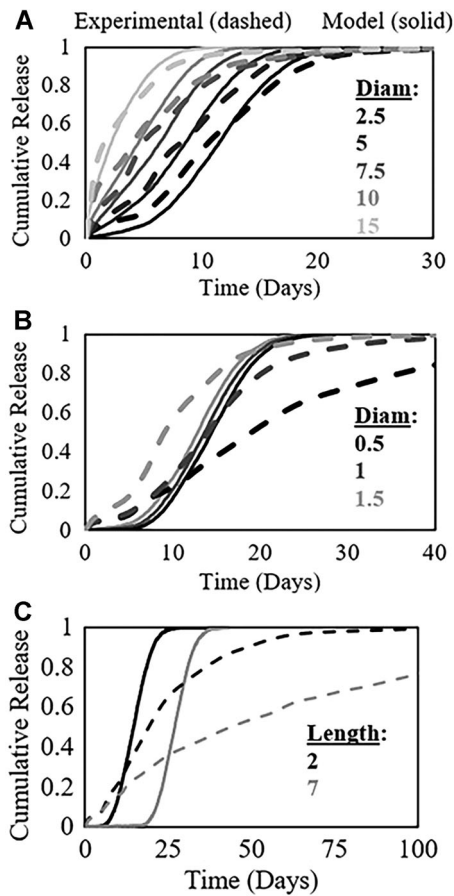


FIGURE 7 Model fit of cumulative release data. A, Model fit (solid lines) of normalized cumulative release data (dashed lines) from reservoirs with channel diameters between 2.5 and 15 mm (Figure 3). B, Model fit of data from reservoirs with diameters between 0.5 and 1.5 mm (Figure 3). C, Model fit of data from reservoirs with 0.5 mm diameter and length of 2 vs 7 mm (Figure 5C)

to treat chronic bone infections. Despite extended elution, the increased length of the X-shaped channels decreased the compressive strength ($P < .0001$) and Young's modulus ($P < .001$) due to the increased void space in the reservoir shell (Figure 10E,F).

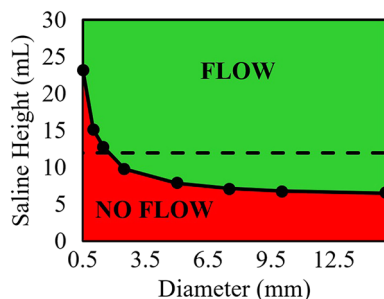


FIGURE 8 Height of saline required for fluid to flow through channels. The dashed line represents approximate saline height used in elution studies for Figures 3-5 [Color figure can be viewed at wileyonlinelibrary.com]

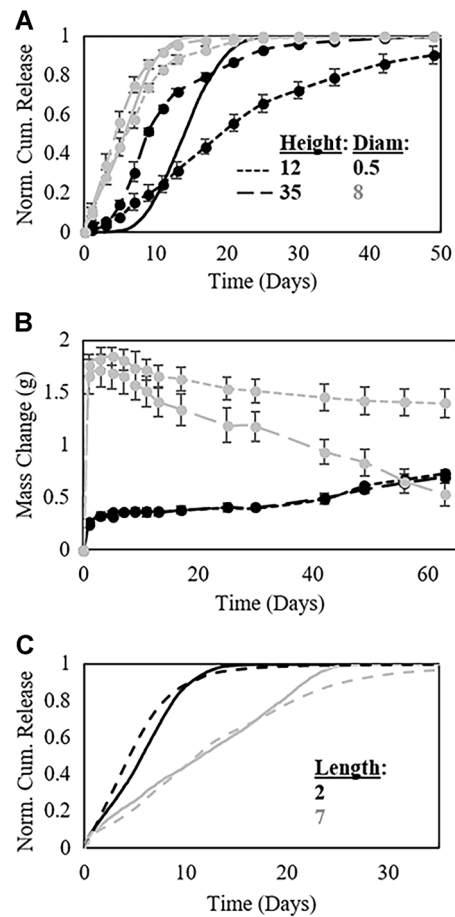


FIGURE 9 Saline height and model prediction. A, Effect of saline height (12 vs 35 mm) on normalized cumulative release for reservoirs with channel diameters 0.5 vs 8 mm compared to the model prediction (solid lines). B, Change in mass over time for the reservoirs in (A). C, Model prediction (solid) and data (dashed) for reservoirs with channel diameter 8 mm and length 2 vs 7 mm

4 | DISCUSSION

Effective treatment for PJI requires a high-strength device that enables load-bearing activity while eluting therapeutic levels of antibiotics for many weeks.^{29,30} Antibiotic-impregnated PMMA spacers only support partial weight-bearing with minimal release of antibiotics over time.¹² In this study, we fabricated a 3D-printed model scaffolds with reservoirs as a depot for the long-term delivery of antibiotics from a biodegradable carrier. Compartmentalizing the mechanical and therapeutic activities via two different materials enables the strength and antibiotic release profile to be independently tuned.

The rate of drug liberation from bioceramics is significantly greater than the resorption rate, so the antibiotic release is mediated primarily by diffusion rather than degradation of the bioceramic.³¹ In order to extend antibiotic elution, reservoirs must be designed to slow the diffusion of the drug through the bioceramic. We demonstrate that reducing the area, or porosity, or increasing the length of 3D-printed channels extend release by forcing antibiotics to diffuse

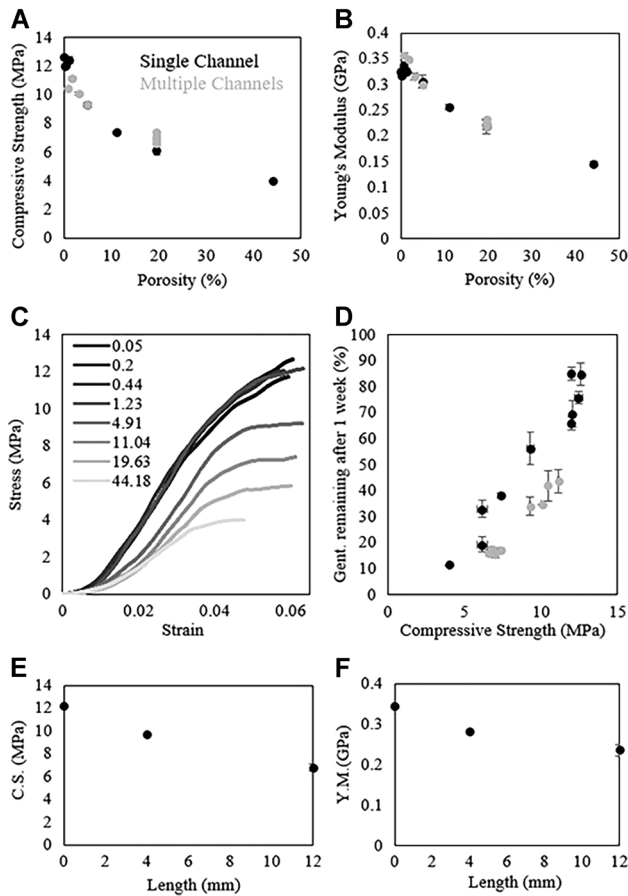


FIGURE 10 Mechanical properties of reservoirs: A, Compressive strength and (B) Young's modulus of reservoirs from Figures 3 and 4. Black data are from reservoirs with a single channel per side and red data are from reservoirs with multiple channels per side. C, Representative stress-strain curves for reservoirs with a single channel per side. The legend refers to the channel porosity. D, Correlation between the percent gentamicin remaining in the reservoir after 1 week vs the compressive strength of the reservoir. E, Compressive strength and (F) Young's modulus of reservoirs from Figure 5E. CS, compressive strength; YM, Young's modulus

further to reach the channels to exit the system. While not the main focus of this study, it is important to note that the interaction between the cement and antibiotic also affects elution. For instance, increasing the liquid-to-powder ratio of the cement will increase the cement porosity and expedite antibiotic diffusion.³² In addition, bioceramics with different degradation rates can also influence drug release. CPC degrade slower than CS cements to prolong antibiotic release.³³ Future studies should explore parameters of the cement and antibiotic mixture on antibiotic elution from reservoirs.

A simple computational model accurately fit antibiotic release data from reservoirs with channels that have diameters greater than 1.5 mm. At lower diameters, the hydrophobic properties of the RPU material could potentially limit the exchange of saline and degraded cement, resulting in a more extended-release profile than predicted by the model. At greater channel diameters, the model can effectively predict the geometry needed to achieve a desired cumulative release

profile. A constant rate of release over many weeks would be ideal to treat an infection. Experimental data confirmed model predictions that an 8-mm channel diameter results in an approximately linear release profile. Increasing the channel length extended the release while maintaining a linear shape.

This study demonstrates that reservoirs have the capacity to release therapeutic levels of antibiotics for longer than spacers are cleared for use by the Food and Drug Administration (180 days). However, a limitation of this study is that in vitro elution studies do not accurately reflect in vivo conditions, so it is difficult to predict how long therapeutic antibiotic concentration would maintain in vivo. We showed that cement degradation increases as the pressure exerted by the fluid increases. Since the pressure of the synovial fluid in an infected joint is difficult to determine, it will be challenging to effectively predict the release profile of antibiotics in vivo. Some studies have shown that in vivo release from bioceramics is slower than in vitro release while other studies show the reverse.³⁴⁻³⁸ The data presented in this study at least provide general knowledge about the factors that influence drug release from reservoirs. Future work should investigate antibiotic release from reservoirs in large animal models of infection.

Material selection for the 3D-printed implant is paramount to tuning the mechanical strength of reservoirs. Without a need for drug-eluting activity, there are multiple materials with greater strength than PMMA that would enable full load-bearing activity. A limitation of this study is that reservoirs were 3D printed with an RPU with a compressive strength of approximately 45 MPa, which is weaker than PMMA and thus limits the final strength of the composite implant. However, the techniques developed from this study can be applied to reservoirs 3D printed from high-strength materials. For instance, others have 3D-printed reservoir-containing devices from titanium using SLM.^{24,25} Titanium is considerably stronger than PMMA and has the potential to support full load-bearing activity during the treatment of PJI.

In addition to enabling load-bearing activity and improving eradication of the infection, a high-strength 3D-printed spacer could significantly reduce the rising costs of treating PJI. PMMA spacers are more expensive than primary implants, so a 3D-printed device could be cheaper than current spacers on the market. Furthermore, due to the high strength of the device, there would be no need for additional surgery to replace the spacer with a new primary implant, which would dramatically save on costs. There is also potential that the local antibiotic release is so effective that the patient would need less systemic antibiotics. As a result, a high-strength 3D-printed device with antibiotic-eluting reservoirs could improve treatment, patient mobility, and satisfaction, and reduce costs significantly.

Overall, this study demonstrates the potential to tune both the mechanical and drug-eluting properties of implants with reservoirs. Optimization of the 3D-printed material, reservoir geometry, and biodegradable carrier can result in a device with substantially improved efficacy vs current PMMA spacers. While this study focuses on the treatment of PJI, the reservoir platform could potentially be applied to other devices. Intramedullary nails are often used to treat

nonunion bone fractures.³⁹ A reservoir-containing intramedullary nail could be loaded with a biodegradable carrier that elutes growth factors to promote bone growth and antibiotics to prevent infection in compound fractures. Reservoir-containing implants can also be used after the excision of cancerous bone tissue as a bone graft substitute that elutes chemotherapeutic while maintaining load-bearing function.²⁴ Understanding the ability to tune the mechanical and drug-eluting properties of reservoirs enables the design of a range of devices that could treat numerous afflictions.

ACKNOWLEDGMENT

This study was supported by the Duke-Coulter translational partnership under Grant Number 291-0067.

AUTHOR CONTRIBUTIONS

BA: substantial contributions to research design, and the acquisition, analysis, and interpretation of data; drafting the manuscript; and approval of the submitted manuscript. CM: Substantial contributions to the acquisition of data and approval of the submitted manuscript. TS: Substantial contributions to research design and the interpretation of data, and approval of the submitted manuscript. KG: Substantial contributions to research design, and the interpretation of data; revising the manuscript; and approval of the submitted manuscript.

ORCID

Brian Allen  <http://orcid.org/0000-0002-1966-2464>

REFERENCES

- Tande AJ, Patel R. Prosthetic joint infection. *Clin Microbiol Rev.* 2014; 27(2):302-345.
- ter Boo GJ, Grijpma DW, Moriarty TF, Richards RG, Eglin D. Antimicrobial delivery systems for local infection prophylaxis in orthopedic- and trauma surgery. *Biomaterials.* 2015;52:113-125.
- Kurtz S, Ong K, Lau E, Mowat F, Halpern M. Projections of primary and revision hip and knee arthroplasty in the United States from 2005 to 2030. *J Bone Joint Surg Am.* 2007;89(4):780-785.
- Kurtz SM, Ong KL, Lau E, Bozic KJ. Impact of the economic downturn on total joint replacement demand in the United States: updated projections to 2021. *J Bone Joint Surg Am.* 2014;96(8):624-630.
- Eckardt JJ, Wirganowicz PZ, Mar T. An aggressive surgical approach to the management of chronic osteomyelitis. *Clin Orthop Relat Res.* 1994;298:229-239.
- Gogia JS, Meehan JP, Di Cesare PE, Jamali AA. Local antibiotic therapy in osteomyelitis. *Semin Plast Surg.* 2009;23(2):100-107.
- Jaeblo T. Polymethylmethacrylate: properties and contemporary uses in orthopaedics. *J Am Acad Orthop Surg.* 2010;18(5):297-305.
- Webb J, Spencer RF. The role of polymethylmethacrylate bone cement in modern orthopaedic surgery. *J Bone Joint Surg Br.* 2007; 89B(7):851-857.
- Goltzer O, McLaren A, Overstreet D, Galli C, McLemore R. Antimicrobial release from prefabricated spacers is variable and the dose is low. *Clin Orthop Relat Res.* 2015;473(7):2253-2261.
- Inzana JA, Schwarz EM, Kates SL, Awad HA. Biomaterials approaches to treating implant-associated osteomyelitis. *Biomaterials.* 2016;81: 58-71.
- Neut D, van de Belt H, van Horn JR, van der Mei HC, Busscher HJ. Residual gentamicin-release from antibiotic-loaded polymethylmethacrylate beads after 5 years of implantation. *Biomaterials.* 2003;24(10):1829-1831.
- Virto MR, Frutos P, Torrado S, Frutos G. Gentamicin release from modified acrylic bone cements with lactose and hydroxypropylmethylcellulose. *Biomaterials.* 2003;24(1):79-87.
- Jiranek WA, Hanssen AD, Greenwald AS. Antibiotic-loaded bone cement for infection prophylaxis in total joint replacement. *J Bone Joint Surg Am.* 2006;88(11):2487-2500.
- Lautenschlager EP, Jacobs JJ, Marshall GW, Meyer PR Jr. Mechanical properties of bone cements containing large doses of antibiotic powders. *J Biomed Mater Res.* 1976;10(6):929-938.
- McConoughey SJ, Howlin RP, Wiseman J, Stoodley P, Calhoun JH. Comparing PMMA and calcium sulfate as carriers for the local delivery of antibiotics to infected surgical sites. *J Biomed Mater Res B Appl Biomater.* 2015;103(4):870-877.
- Inzana JA, Trombetta RP, Schwarz EM, Kates SL, Awad HA. 3D printed bioceramics for dual antibiotic delivery to treat implant-associated bone infection. *Eur Cell Mater.* 2015;30:232-247.
- Zilberman M, Elsner JJ. Antibiotic-eluting medical devices for various applications. *J Controlled Release.* 2008;130(3):202-215.
- Loca D, Sokolova M, Locs J, Smirnova A, Irbe Z. Calcium phosphate bone cements for local vancomycin delivery. *Mater Sci Eng C Mater Biol Appl.* 2015;49:106-13.
- Su WY, Chen YC, Lin FH. A new type of biphasic calcium phosphate cement as a gentamicin carrier for osteomyelitis. *Evid Based Complement Alternat Med.* 2013;2013:801374.
- Stallmann HP, Faber C, Bronckers AL, Nieuw Amerongen AV, Wuisman PI. In vitro gentamicin release from commercially available calcium-phosphate bone substitutes influence of carrier type on duration of the release profile. *BMC Musculoskelet Disord.* 2006;7:18.
- Bohner M, Lemaître J, Merkle HP, Gander B. Control of gentamicin release from a calcium phosphate cement by admixed poly(acrylic acid). *J Pharm Sci.* 2000;89(10):1262-1270.
- Howlin RP, Winnard C, Frapwell CJ, et al. Biofilm prevention of gram-negative bacterial pathogens involved in periprosthetic infection by antibiotic-loaded calcium sulfate beads in vitro. *Biomed Mater.* 2016; 12(1):015002.
- Stigter M, Bezemer J, de Groot K, Layrolle P. Incorporation of different antibiotics into carbonated hydroxyapatite coatings on titanium implants, release and antibiotic efficacy. *J Control Release.* 2004;99(1):127-137.
- Cox SC, Jamshidi P, Eisenstein NM, et al. Adding functionality with additive manufacturing: fabrication of titanium-based antibiotic eluting implants. *Mater Sci Eng C Mater Biol Appl.* 2016;64:407-415.
- Bezuidenhout MB, van Staden AD, Oosthuizen GA, Dimitrov DM, Dicks LMT. Delivery of antibiotics from cementless titanium-alloy cubes may be a novel way to control postoperative infections. *BioMed Res Int.* 2015;2015:856859.
- Bezuidenhout MB, Booyesen E, van Staden AD, et al. Selective laser melting of integrated Ti6Al4V ELI permeable walls for controlled drug delivery of vancomycin. *ACS Biomater Sci Eng.* 2018;4(12):4412-4424.
- van de Belt H, Neut D, Schenk W, van Horn JR, van der Mei HC, Busscher HJ. Gentamicin release from polymethylmethacrylate bone cements and Staphylococcus aureus biofilm formation. *Acta Orthop Scand.* 2000;71(6):625-629.
- Aiken SS, Cooper JJ, Florance H, Robinson MT, Michell S. Local release of antibiotics for surgical site infection management using high-purity calcium sulfate: an in vitro elution study. *Surg Infect.* 2015;16(1):54-61.
- Bejon P, Berendt A, Atkins BL, et al. Two-stage revision for prosthetic joint infection: predictors of outcome and the role of reimplantation microbiology. *J Antimicrob Chemother.* 2010;65(3):569-575.
- Kapadia BH, Berg RA, Daley JA, Fritz J, Bhav A, Mont MA. Periprosthetic joint infection. *Lancet.* 2016;387(10016):386-394.
- Ginebra MP, Canal C, Espanol M, Pastorino D, Montufar EB. Calcium phosphate cements as drug delivery materials. *Adv Drug Deliv Rev.* 2012;64(12):1090-1110.
- Otsuka M, Matsuda Y, Fox JL, Higuchi WI. A novel skeletal drug delivery system using self-setting calcium phosphate cement. 9:

- effects of the mixing solution volume on anticancer drug release from homogeneous drug-loaded cement. *J Pharm Sci.* 1995;84(6): 733-736.
33. Ferguson J, Diefenbeck M, McNally M. Ceramic biocomposites as biodegradable antibiotic carriers in the treatment of bone infections. *J Bone Jt Infect.* 2017;2(1):38-51.
34. Parent M, Baradari H, Champion E, Damia C, Viana-Trecant M. Design of calcium phosphate ceramics for drug delivery applications in bone diseases: a review of the parameters affecting the loading and release of the therapeutic substance. *J Control Release.* 2017;252:1-17.
35. Uchida A, Shinto Y, Araki N, Ono K. Slow release of anticancer drugs from porous calcium hydroxyapatite ceramic. *J Orthop Res.* 1992; 10(3):440-445.
36. Iannuccelli V, Coppi G, Bondi M, Pinelli M, Mingione A, Cameroni R. Biodegradable intraoperative system for bone infection treatment II. In vivo evaluation. *Int J Pharm.* 1996;143(2):187-194.
37. Baro M, Sanchez E, Delgado A, Perera A, Evora C. In vitro-in vivo characterization of gentamicin bone implants. *J Control Release.* 2002; 83(3):353-364.
38. Castro C, Evora C, Baro M, Soriano I, Sanchez E. Two-month ciprofloxacin implants for multibacterial bone infections. *Eur J Pharm Biopharm.* 2005;60(3):401-406.
39. Shyam AK, Sancheti PK, Patel SK, Rocha S, Pradhan C, Patil A. Use of antibiotic cement-impregnated intramedullary nail in treatment of infected non-union of long bones. *Indian J Orthop.* 2009;43(4):396-402.

SUPPORTING INFORMATION

Additional supporting information may be found online in the Supporting Information section.

How to cite this article: Allen B, Moore C, Seyler T, Gall K. Modulating antibiotic release from reservoirs in 3D-printed orthopedic devices to treat periprosthetic joint infection. *J Orthop Res.* 2020;38:2239-2249.

<https://doi.org/10.1002/jor.24640>